Supporting Information

Magnetite/Graphene Nanosheet Composites: Interfacial Interaction and Its Impact on the Durable High-Rate Performance in Lithium-Ion Batteries

Jisheng Zhou[1], *Huaihe Song*[1*], *Lulu Ma*[1, 2], *Xiaohong Chen*[1]

1 State Key Laboratory of Chemical Resource Engineering, Key Laboratory of Carbon Fiber and Functional Polymers, Ministry of Education, Beijing University of Chemical Technology, Beijing, 100029 P. R .China

2 Mechanical Engineering and Materials Science, Rice University, Houston TX 77005, USA

* Corresponding author, E-mail: songhh@mail.buct.edu.cn

Table S1. Comparison of the electrochemical performance of Graphene/Fe3O4 composite nanosheets synthesized in this work with those of graphene/metal oxide composites reported in the literatures

Samples	Graphene content (%)	Current density	Reversible capacity(mAhg^{-1})	Cycle number	Capacity retention (mAhg^{-1})	Reference
SnO_2	--	50 mAg^{-1}	810	30	570	(1)
Sn	65	55 mAg^{-1}	810	100	508	(2)
SnO_2	40	C/5	786	50	558	(3)
Co_3O_4	34	74 mAg^{-1}	754	20	760	(4)
		1860 mAg^{-1}	500	10	--	
Co_3O_4	24.6	50 mAg^{-1}	800 (for the 5th cycle)	30	935	(5)
		500 mAg^{-1}	484	--	--	
Co_3O_4	46.2	89 mAg^{-1}	1086 (for the 3rd cycle)	30	1065	(6)
CuO		65 mAg^{-1}	ca. 600	100	ca. 600	(7)
		1600 mAg^{-1}	320	5	--	
		6400 mAg^{-1}	150	5	--	
Mn_3O_4		40 mAg^{-1}	ca.900	5	ca.900	(8)
		400 mAg^{-1}	ca. 780	10	ca. 780	
		1600 mAg^{-1}	ca. 390	10		
Fe_3O_4	38	100 mAg^{-1}	664	100	650	(9)
Fe_3O_4	13.30%	35 mAg^{-1}	922	30	1026	(10)
		700 mAg^{-1}	ca. 600	100	ca. 540	
		1750 mAg^{-1}	520	10	--	
Fe_3O_4	22.7	100 mAg^{-1}	1060	40	1048	(11)
		300mAg^{-1}	740	10	--	
		500mAg^{-1}	600	10	--	
		1000 mAg^{-1}	410	10	--	
Fe_3O_4	--	C/10	870	50	650	(12)
		1C	700	--	--	
		5C	350	--	--	
Fe_3O_4	33	C/5	755.6	30	538.7	(13)
Fe_3O_4	30	50 mAg^{-1}	825	50	951	this work
		500 mAg^{-1}	730	200	796	
		1000 mAg^{-1}	550	300	531	
		2000 mAg^{-1}	523	300	335	
		5000 mAg^{-1}	491	300	213	

(1) S.-M. Paek, E.Yoo and I. Honma, *Nano Lett.* 2009, **9**, 72-75.

(2) G. Wang, B. Wang, X. Wang, J. Park, S. Dou, H. Ahn and K. Kim, *J. Mater. Chem.* 2009, **19**, 8378-8384.

(3) L.-S. Zhang, L.-Y. Jiang, H.-J. Yan, W. D. Wang, W. Wang, W.-G. Song, Y.-G. Guo, L.-J. Wan, *J. Mater. Chem.* 2010, **20**, 5462-5467.

(4) S. Yang, G. Cui, S. Pang, Q. Cao, U. Kolb, X. Feng, J. Maier and K. Müllen, *ChemSusChem,* 2010, **3**, 236-239.

(5) Z.-S. Wu, W. Ren, L. Wen, L. Gao, J. Zhao, Z. Chen, G. Zhou, F. Li, H.-M. Cheng, *ACS Nano,* 2010, **6**, 3187-3194.

(6) S. Q. Chen and Y. Wang, *J. Mater. Chem.,* 2010, **20**, 9735-9739.

(7) Wang, B.; Wu, X.-L.; Shu, C.-Y.; Guo, Y.-G.; Wang, C.-R. *J. Mater. Chem.* **2010**, *20*, 10661-10664.

(8) H. Wang, L.-F. Cui, Y. Yang, H. S. Casalongue, J. T. Robinson, Y. Liang, Ycui and H. Dai, *J. Am. Chem. Soc.,* 2010, **132**, 13978-13980.

(9) J.-Z. Wang, C. Zhong, D. Wexler, N. H. Idris, Z.-X. Wang, L.-Q. Chen and H.-K. Liu, *Chem. Eur. J.* 2011, **17**, 661-667.

(10) G. Zhou, D.-W. Wang, F. Li, L. Zhang, N. Li, Z.-S. Wu, L. Wen, G. Q. Lu and H.-M. Chen, *Chem. Mater.,* 2010, **22**, 5306-5313.

(11) P. Lian, X. Zhu, H. Xiang, Z. Li, W. Yang and H. Wang, *Electrochim. Acta,* 2010, **56**, 834-840.

(12) M. Zhang, D. Lei, X. Yin, L. Chen, Q. Li, Y. Wang and T. Wang, *J. Mater. Chem.,* 2010, **20**, 5538-5543.

(13) B. Li, H. Cao, J. Shao, M. Qu and J. H. Warner, *J. Mater. Chem.,* 2011, **21**, 5069-5075.

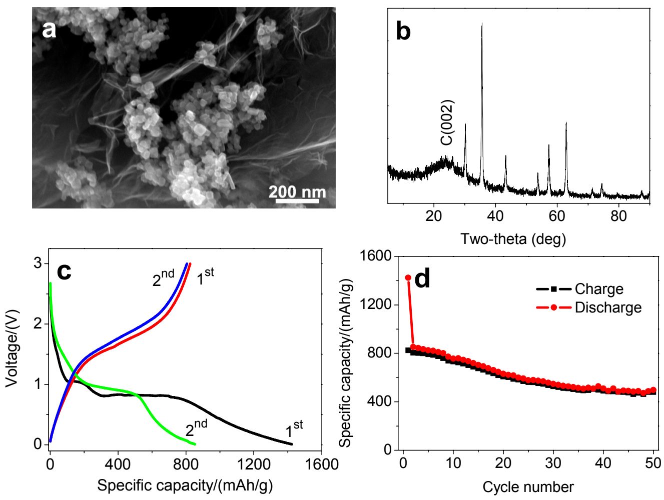

Figure S1. (a) SEM image and (b) XRD pattern of Fe_3O_4/graphene composite prepared by simple mechanical blending without ultrasonication, and the corresponding electrochemical performance used as anode materials for lithium-ion batteries: (c) initial two charge-discharge curves and (d) cyclic performance measured at a current density of 50 mA/g between 0.01 and 3.0 V.

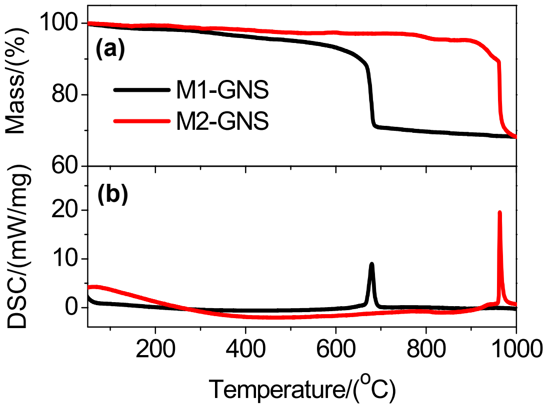

Figure S2. (a) TG and (b) DSC curves of M1-GNS and M2-GNS at the Ar atmosphere.

Table S2 Data for Raman spectra

Sample	$C_D/(cm^{-1})$	$C_G/(cm^{-1})$	I_D/I_G
GNS	1349	1583	0.93
M2-GNS	1343	1583	0.93
M1-GNS	1342	1592	1.04
Graphene from M1-GNS	1345	1585	1.03

Note: C_D and C_G stand for the center wave numbers of D- and G-peak, respectively. And I_D/I_G is (are) the intensity ratio of D- and G-peak, respectively.

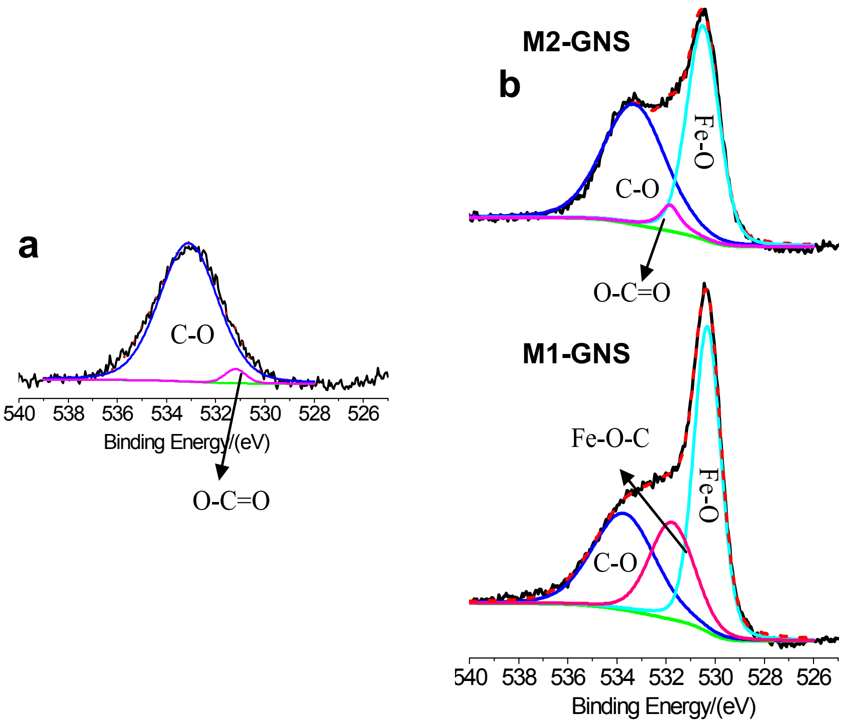

Figure S3. XPS spectrum of O1s in (a) graphene sheets obtained after removing Fe_3O_4 from M1-GNS, and (b) O1s spectra of M1-GNS and M2-GNS: from the Figure (b), it can be seen obviously that a new peak at ca. 531.7 eV presences in the spectrum of M1-GNS, which is not in M2-GNS.

Table S3. Binding energy of O1s in various bonds

C-O bond	B.E./(eV)	Metal-O bond	B.E./(eV)	Metal-O-C bond	B.E./(eV)
		Fe_3O_4	530 [14]	Fe-O-C	ca. 531 [15]
					532.3 [16]
					533 [16]
epoxy		CuO	529.6 [14]	Cu-O-C	532.8 [17]
C-O-C in		AgO	528.6 [14]	Ag-O-C	531.7 [18]
graphene	533	ZrO_2	530.2 [14]	Zr-O-C	532±0.2 [19]

(14) Moulder, J. F.; Stickle, W. F.; Sobol, P. E.; Bomben, K. D. Handbook of X-ray Photoelectron Spectroscopy, published by Perkin-Elmer Corp., 1992, Eden Prairie, MN, USA

(15) Kataby, G.; Cojocaru, M.; Prozorov, R.; Gedanken, A. Coating carboxylic acids on amorphous iron nanoparticles. *Langmuir* **1999**, *15*, 1703.

(16) Combellas, C.; Delamar, M.; Kanoufi, F.; Pinson, J.; Podvorica, F. I. Spontaneous grafting of iron surfaces by reduction of aryldiazonium salts in acidic or neutral aqueous solution application to the protection of iron against corrosion. *Chem. Mater.* **2005**, *17*, 3968.

(17) Hurley, B. L.; McCreery, R. L. Covalent bonding of organic molecules to Cu and Al alloy 2024 T3 surfaces via diazonium ion reduction. *J. Electrochem. Soc.* **2004**, *151*, B252.

(18) Serghini-Monim, S.; Norton, P. R.; Puddephatt, R. J.; Pollard, K. D.; Rasmussen, J. R. *J. Phys. Chem. B* **1998**, *102*, 1450.
(19) Dicke, C.; Morstein, M.; Hahner, G. Surface inorganic chemistry: the reaction of hydroxyl-terminated thiols on gold with a zirconium coordination compound. *Langmuir* **2002**, *18*, 336.

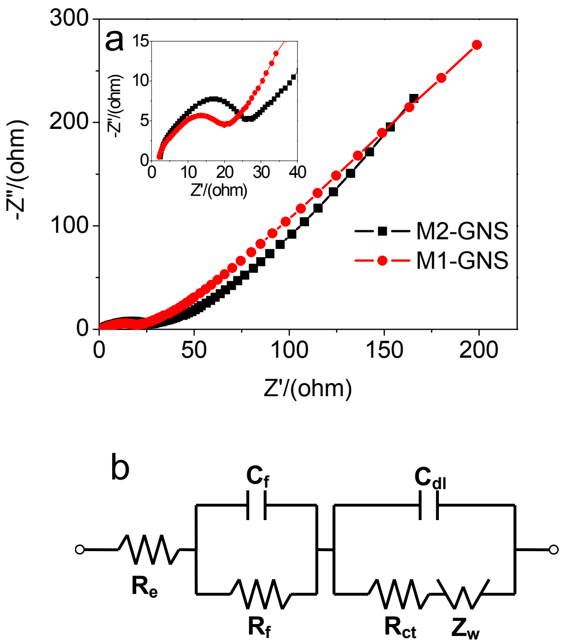

Figure S4. (a) AC impedance of M1- and M2-GNS after 4 cycles at 50 mAg^{-1}, and (b) randles equivalent circuit.

From Figure S4a, the Nyquist plots of M1- and M2-GNS consist of a depressed semicircle in high- and middle-frequency regions and a straight line in the low-frequency region. The linear region is attributed to the semi-infinite diffusion of Li ions in the electrode materials, whereas the depressed semicircle can be interpreted as arising from SEI film and contact resistance in high frequency, and charge-transfer process in mid-frequency, respectively. [20] The diameter of semicircle for M1-GNS is smaller than that of M2-GNS, indicating that M1-GNS owns the lower surface film and charge-transfer resistances. To obtain the quantitative analysis, the EIS is modeled by an equivalent circuit shown in Figure S5b. [20] R_e is the electrolyte resistance. C_f and R_f are the capacitance and resistance of the surface film formed on the electrodes, respectively. C_{dl} and R_{ct} are the double-layer capacitance and charge-transfer resistance, respectively. Z_w is the Warburg impedance related to the diffusion of lithium ions into the bulk electrodes.

(20) a) Yang, S.; Huo, J.; Song, H.; Chen, X. Electrochemical Performance of Expanded Mesocarbon Microbeads as Anode Material for Lithium-Ion Batteries. Electrochem. Commun. 2006, 8, 137-142. b) Zhou, J.; Song, H.; Fu, B.; Wu, B.; Chen, X. Synthesis and High-rate Capability of Quadrangular Carbon Nanotubes with One Open End as Anode Materials for Lithium-Ion Batteries. J. Mater. Chem. 2010, 20, 2794-2800.

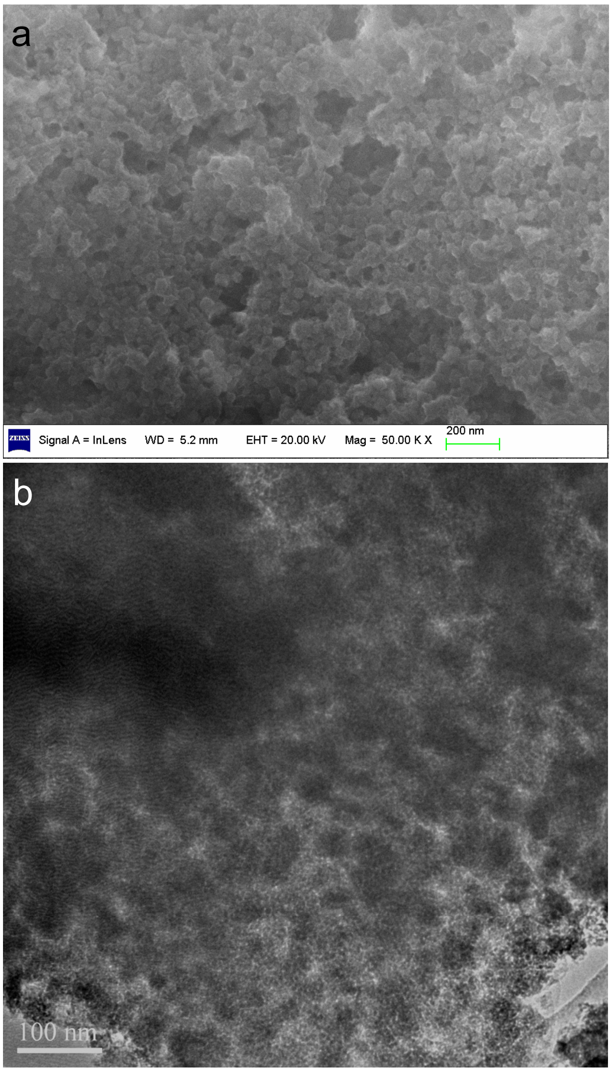

Figure S5. a) SEM and b) TEM images of M1-GNS electrode after the 200th cycles at 500 mAg^{-1}.